A Simplified Numerical Model for a Flat Continuous Triangle Fins Air Cooled Heat Exchanger Using a Step by Step Technique

Dr. Ali Hussain Tarrad
Mech. Eng. Dept
College of Engineering
Al-Mustansiriya University
Baghdad-Iraq

Dr. Fouad Alwan Saleh
Mech. Eng. Dept
College of Engineering
Al-Mustansiriya University
Baghdad-Iraq

Ali Ahmed Abdulrasool
Mech. Eng. Dept
College of Engineering
Al-Mustansiriya University
Baghdad-Iraq

Abstract

This investigation deals with the performance prediction of cross flow air cooled heat exchangers. An experimental work was carried out on a finned tube air cooled heat exchanger. A water supplying system rig was built for this object which provides water at temperature range of (10 to 50) °C with water circulating rate up to (2000) l/hr. Air volumetric flow rates of (500,1000 and 2000) cfm at a temperature of (32) ºC was used during the experiments. A two dimensional model was suggested to perform the core dimensions prediction of the air cooled heat exchanger. This model was based on the step by step technique which is suggested to divide the height and depth dimensions of the heat exchanger to slices and rows respectively. The thermal performance represented by heat load, heat transfer coefficient (air side), overall heat transfer coefficient and air exit temperature from heat exchanger were predicted by the present model. The suggested simulation model showed that the maximum discrepancy between the predicted and experimental values of the heat exchanger performance was about (3 %).

الخلاصـــــة

البحث الحالي يَتعاملُ مع التنبؤ بأداءِ المبادلات الحرارية المبّردة بالهواء ذات الجريان المتقا ـع . تم إجراء الجانب العملي من هذا البحث على مبادل ذو أنابيب مزعنفة مبرد بالهواء. تم بناء منظومة مختبريه تقوم بتجهيز الماء بدرجات حرارة تتراوح بين (10) و (50) م° وبمعدل جريان يصل إلى (2000) لتر/ساعة . التجارب العملية تم تنفيذها لثلاث قيم لمعدل حجمي لجريان الهواء هي (500), (1000) و(2000) قدم3/دقيقة بدرجة حرارة (32) م° . تم بناء نموذج رياضي ثُنائي الإبعاد للتنبؤ بالإبعاد الفيزياوية للمبادل الحراري المبرد بالهواء. يعتمد النموذج على تقنية مبدأ الخطوة-خطوة والتي عند تطبيقها تم تقسيم السمك والارتفاع للمبادل إلى صفوف و شرائح على التوالي. تم التنبؤ

باستخدام النموذج الحالي بالأداء الحراري للمبادل متمثلاً بالحمل الحراري, معامل انتقال الحرارة لجانب الهواء, معامل انتقال الحرارة الكلي ودرجة حرارة الهواء الخارج من المبادل الحراري. لقد بين النموذج المقترح إن اكبر فرق بين النتائج العملية والقيم المحسوبة لأداء المبادل الحراري كان بحدود (3) ٪.

1. Introduction

Compact heat exchangers have been widely used in various applications in thermal fluid systems including automotive thermal management systems. Radiators for engine cooling systems, evaporators and condensers for *HVAC* systems, oil coolers, and intercoolers are typical examples of the compact heat exchangers that can be found in ground vehicles. Generally, the main object of compact heat exchanger is the large heat transfer area relative to the size.

Ganapathy (1979) [1] concluded that for air- cooled condensers ambient air is the most important variable in the design. Since ambient temperature in a location varies throughout the year, a higher value, if used, would result in over sizing the unit .A lower value would give poor performance. Current practice is to use a design temperature that exceeds (2 to 5) % of the annual period.

Hedderich and Kellehere (1982)[2] developed a computer code for the analysis of air cooled heat exchangers and was coupled with a numerical optimization program to produce an automated air cooled ,heat exchanger design and optimization procedure. A general iteration free approximation method was used for the analysis which calculates the mean overall heat transfer coefficient and the overall pressure drop for many arrangements.

The analysis takes into account the variation of heat transfer coefficients and the pressure drop with temperature and length of flow path .The capability is demonstrated by the design of an air cooled finned tube heat exchanger and is shown to be useful tool for heat exchanger design.

Matthew and Joseph (2002) [3] developed a conceptual designs for wet and dry cooling systems as applied to a new, gas –fired, combined cycle 500-*MW* plant at four sites chosen to be representative of conditions in California. Cooling system power requirements for dry systems are four to six times those for wet systems. Dry systems, which are limited by the ambient dry bulb temperature, cannot achieve as low a turbine back pressure as wet systems, which are limited by the ambient wet bulb.

Dohoy and Dennis (2006)[4] divided the heat exchanger core into small control volumes along the tube. Finite Difference Method (FDM) with staggered grid system was employed in their numerical model. FDM enables us to take into account the significant air temperature increase as well as the local variations of the properties and the heat transfer coefficient. The maximum difference between the experimental data and calculated results is (5%) for the given range of the simulated conditions.

More recently, Tarrad, et al. (2008) [5] investigated the performance prediction of the cross flow air-cooled heat exchanger. They developed a new simplified correlation for the air

side heat transfer coefficient depended on the dimensional analysis with Buckingham-pi theorem. The discrepancy between the predicted and experimental values of the overall heat transfer coefficient and heat duty were within 2% and 4% respectively for both of the tested tube banks.

In the present study a step by step technique is applied to find out the thermal design of the single pass air cooled heat exchanger. The work was verified by experimental data obtained through a closed circuit built for this object. A computer program model was built for this purpose to incorporate the idea of the step by step method suggested in this study.

2. Test Rig

The experimental rig is a modification of an existing apparatus available in the laboratory developed previously by Tarrad and Mohammed (2006) [6]. The cold water is supplied by a constant head tank of (200) liters capacity. The water is pumped by a single stage centrifugal pump from tank through the test section and it returns back to the tank. The water in the hot tank is heated by four electrical heaters, which have a total heating electrical power of (12) *kW*. The four heaters are fixed in the same level at (150) *mm* from the bottom of the hot tank and separated at (90°) apart. The hot tank is opened into cold tank by gate valve which is fixed in the pipe that linked the two tanks, as shown in figure (1). This arrangement will assure an acceptable control of the water temperature during tests. The mixing of water was allowed to be in the cold tank to get the set required temperature. The ice was immersed into the cold tank to obtain a homogenous water mixture before pumping through the heat exchanger test section.

2-1 Heat Exchanger Test Section

The test section is made of compact heat exchanger of two rows, cross-flow exchanger with both fluids unmixed. Edges of flat vertical tubes, of dimensions (55) *cm* length, (3.5) *cm* depth and (37) *cm* height, the heat exchanger geometry specifications are illustrated in table (1). The compact heat exchanger configuration is shown in figure (2), in which the water flows in the tubes in cross flow direction to the air that flows normal to tubes. Thermometers gauges are connected to the heat exchanger. The gauges are fixed in specially prepared pockets mounted on the required locations.

2-2 Air Circulation System

The air was supplied to the test heat exchanger through a centrifugal fan. A forced draught arrangement was selected for the test object by variable fan speed. Three volumetric flow rates was tested of capacities of (2000) *cfm* and (1000) *cfm*. Further an axial fan was used to provide a flow rate of (500) *cfm*. The fan was installed close enough to the test section

to avoid leakage of air to the surrounding. The air volumetric flow rate is measured by using a Pitot-tube measuring device.

3. Variables Measured and Instrumentation

The parameters to be measured during the test are:

1. The inlet and outlet temperatures of the heat exchanger for both air and water streams.
2. The air flow rate across the heat exchanger.
3. The water flow rate in the tube side.

Thermocouples of the (K) type having a range of (0 – 120) $^{\circ}C$, are used to measure the temperatures at inlet and outlet of heat exchanger. Two pointer pressure gauges installed on both sides of heat exchanger to measure the pressure of the water and have a range of (0 – 2.5) *bar*, which are connected to the heat exchanger. Two vertical GEC Elliott type variable area rotameters were used to measure the flow rates of the water for the range of (200 – 3000) *l/h*.

4. Numerical Method

In order to develop a numerical model with the predictive capability for various design parameters of the heat exchanger, the marching technique (step by step) method with two dimensions was employed in this study. Each tube row was divided into a number of horizontal slices occupying the total length of the heat exchanger and for air side the exit of one row is considered as inlet to the next row as shown in figure (3). The marching technique enables the model to take into account the air temperature variation as well as the local variations of the properties and the heat transfer coefficient. Forms of the mass and the energy conservation equations were derived for two dimensional grid systems.

In the present study the following assumptions were assumed to be existed;

1. Homogenous temperature distribution for air all over the frontal face area of the heat exchanger and hence for each slice.
2. Uniform mass flow distribution for both stream sides of heat exchanger.
3. The exit air condition for each row represents a mean value for all of the slices of the considered row. This will be considered as the inlet condition for the next row.
4. The inlet air velocity for each row was assumed to be uniform represented by a mean representative value.
5. The water temperature variations between the rows were also assumed to be negligible.

4-1 Introductory to Heat Exchanger Design

From the selected velocity of the tube side of the water stream and the known tube cross section dimension, the total number of tubes of the heat exchanger can be calculated from:

$$(N_t) = [\frac{\dot{V}_w}{N_r \times v_w \times A_{cw}}] \quad \text{.....(1)}$$

This value will be used for the estimation of the length and depth of the heat exchanger as:

$$L = X_T \times (N_t + 1) \quad \text{.....(2)}$$

$$D = [X_L \times (N_r - 1)] + D_t \quad \text{.....(3)}$$

4-2 Mass Conservation

Mass conservation of the water flow through the tube is simply

$$\Sigma \dot{m}_{in} - \Sigma \dot{m}_{out} = 0 \quad \text{.....(4)}$$

and the mass conservation equation for the water at each slice can be written as:

$$\dot{m}_w(i+1,j) = \dot{m}_w(i,j) \quad \text{.....(5)}$$

In case of the heat exchangers with plain continuous fins, the mass flow rate in the air flow direction can be calculated by the following equation.

$$\dot{m}_a(i,j) = \dot{m}_a(i,j+1) \quad \text{.....(6)}$$

4-3 Log-Mean Temperature Difference:

To estimate the true mean temperature difference (ΔT_m) between the two fluids. The following relations may be used for the estimation of the logarithmic mean temperature difference according to counter flow directions, Smith [7]:

$$LMTD(i,j) = \frac{(T_a(i,j) - T_w(i,j+1)) - (T_a(i+1,j) - T_w(i,j))}{\ln \frac{(T_a(i,j) - T_w(i,j+1))}{(T_a(i+1,j) - T_w(i,j))}} \quad \text{.....(7)}$$

The actual temperature difference of a cross flow compact heat exchanger is obtained by applying a correction factor (F) to the ($LMTD$) value as, Hewitt [8]:

$$\Delta T_m = F * LMTD \quad \text{.....(8)}$$

where:

$$F = \frac{\sqrt{(R^2+1)} \ln (1-S)/(1-RS)}{(R-1)\ln[\frac{2 - S[R+1-\sqrt{(R^2+1)}]}{2 - S[R+1+\sqrt{(R^2+1)}]}} \quad \text{.....(8a)}$$

$$R = \frac{(T_h(i,j) - T_h(i+1,j))}{(T_c(i.j+1) - T_c(i,j))} \quad \text{.....(8b)}$$

$$S = \frac{(T_c(i,j+1) - T_c(i,j))}{(T_h(i,j) - T_c(i,j))} \quad \text{.....(8c)}$$

4-4 Heat Load

The heat load passes through a control volume on the water side is:

$$Q(i,j) = \dot{m}(i,j) \times Cp(i,j) \times \Delta T(i,j) \quad \text{.....(9)}$$

It can be expressed with the overall heat transfer coefficient, $U(i,j)$, as follows:

$$Q(i,j) = U(i,j) \times A_t \times (i,j) \times \Delta T_m(i,j) \quad \text{.....(10)}$$

The above equation may be applied for all slices per one row.

4-5 Overall Heat – Transfer Coefficient (Uo):

The local overall heat transfer coefficient for each slice based on the outside tube area can be written as follows Holman [9]:

$$U_o(i,j) = \frac{1}{[(\frac{1}{h_a(i,j) \times \eta_o}) + (\frac{t_t}{K_t(A_{in}/A_{out})}) + (\frac{1}{h_w(i,j) \times (A_{in}/A_{out})}) + (\frac{1}{h_{fw} \times (A_{in}/A_{out})})]} \quad \text{....(11)}$$

4-6 Forced Convection Inside Tube:

Numerous relations have been proposed for predicting fully developed turbulent flow in tubes. The popular Dittus-Boelter equation, Dittus-Boelter [10] is given in the form:

$$h_w = 0.023 \ \mathrm{Re}^{0.8} \ \mathrm{Pr}^{n} \ (\frac{k}{d_h}) \quad \text{..... (12)}$$

and cross flow area for water side, rectangular tube with semi circular ends:

$$A_{cw} = [(H_t - t_t) \times (D_t - H_t)] + [(H_t - t_t)^2 \times \pi] \quad \text{.....(13)}$$

also

$$\mathrm{Re} = \frac{\rho v d_h}{\mu} \quad \text{.....(14)}$$

$$d_h = \frac{4 \times A_{cw}}{\lambda_t} \quad \text{.....(15)}$$

where the range of Reynolds $6000 \leq Re \leq 10^7$ and Prandtl $0.5 \leq Pr \leq 120$. The coefficient (0.023) is recommended by McAdams (1954) [11] in place of (0.0243) originally given by Dittus-Boelter. Also, $n = 0.4$ for heating and $n = 0.3$ for cooling.

4-7 Forced Convection for Air Side

The entrance length for the development of the longitudinal velocity profile and the temperature profile is about 10 times the hydraulic diameter. This criterion is particularly valid for calculating the time-averaged coefficient for fluids (air and water) [12] . There are several empirical relationships for heat transfer between the duct surface and the fully

developed flow, the analytical form of these relationships is based on exploiting the analogy between momentum and heat transfer. The popular Dittus-Boelter, eq.(12), is also used for fully developed turbulent flow for air side by using the appropriate variables.

For laminar flow, the Sieder and Tate [13] correlation can be used.

$$h_a = 1.86(\mathrm{Re}\,\mathrm{Pr})^{0.3}\left(d_{ha}/D_f\right)^{0.3}(\frac{k}{d_{ha}}) \qquad \text{.....(16)}$$

where cross flow area for air side:

$$A_{ca} = (\frac{P_f}{2}) \times (X_T - H_t) \qquad \text{.....(17)}$$

The hydraulic diameter for the air side:

$$d_{ha} = \frac{4 \times A_{ca}}{\lambda_f} \qquad \text{.....(18)}$$

The number of slices (*Ni*) depends on the water temperature difference along the tube. A uniform distribution for the air mass flow rate across frontal area of the heat exchanger proportional to the size of the slice was assumed. An iterative scheme was applied to find out the mass flow rate for each slice. The Reynolds number of air side for each slice of the heat exchanger is represented by:

$$G_a = \frac{\dot{m}_a(i,j)}{(A_{ca})} \qquad \text{.....(19)}$$

$$\mathrm{Re}_a(i,j) = \frac{(d_{ha} \times G_a)}{\mu_a(i,j)} \qquad \text{..... (20)}$$

By assuming that there is no temperature gradient between the tubes that share the fins then the fin can be considered to be insulated at the center. Therefore fin efficiency (η_f) can be calculated as that for the case with an adiabatic tip, Briggs [14]:

$$\eta_f = \frac{\tanh(m \times (\frac{L_f}{2}))}{m \times (\frac{L_f}{2})} \qquad \text{..... (21)}$$

where:

$$m = \sqrt{[\frac{(h_a(i,j)(P_f)}{(k_t\, A_{ca})}} \qquad \text{..... (22)}$$

The overall surface fin efficiency is defined by:

$$\eta_o = 1 - [(\frac{A_f}{A}) \times (1 - \eta_f)] \quad \text{..... (23)}$$

where:

$$\frac{A_f}{H} = (L_f \times D_f \times 4) \times (\frac{1}{P_f}) \quad \text{..... (24)}$$

$$\frac{A_{\exp}}{H} = [((\pi \times H_t) + ((D_t - H_t) \times 2) - (2 \times t_f)] \times (\frac{1}{P_f}) \quad \text{..... (25)}$$

$$\frac{A}{H} = (\frac{A_f}{H}) + (\frac{A_{\exp}}{H}) \quad \text{..... (26)}$$

The height for each slice, $H(i,j)$, of the heat exchanger can be calculated from the general form of the heat duty of that slice in the following form:

$$H(i,j) = \frac{Q(i,j)}{U_o(i,j) \times A \times F \times LMTD(i,j)} \quad \text{.....(27)}$$

In which the heat load of the slice is calculated form the water mass flow rate, temperature difference of the slice and the local specific heat of water there according to the mean temperature.

4-8 Power Consumed by the Fan:

The pressure drop across heat exchanger can be calculated from the general pressure drop relationship, London [15], which is most often written in terms of hydraulic diameter,

$$\Delta P = (\rho \frac{v_a^{\ 2}}{2}) * f \frac{D_f}{d_{ha}} \quad \text{.....(28)}$$

To calculate ΔP, the friction factor f must be known and it can be estimated from the flow solution. The friction factors derived from the Colburn [16] flows described by eq. (29) for the fully developed laminar flow:

$$f = \frac{64}{Ra} \ldots \quad \text{.....(29)}$$

is used, hence, turbulent flow is presented in this work.

For isosceles triangular ducts, Bhatti and Shah(1987)[17] recommend, for fully-developed turbulent flow:

$$f = \frac{0.078}{(Ra)^{0.25}} \quad \text{.....(30)}$$

The power consumed by the motor of the fan is estimated from:

$$P_{fan} = \frac{\dot{V}_{air}\,\Delta p}{\eta_{fan}} \qquad \text{.....(31)}$$

where

$$\dot{V}_{air} = \frac{\dot{m}_{air}}{\rho_{air}} \qquad \text{.....(32)}$$

Thus,

$$P_{motor,fan} = \frac{P_{fan}}{\eta_{motor,fan}} \qquad \text{.....(33)}$$

5. Results and Discussion:

The results of the simulation program will be discussed, including the heat load, heat transfer coefficient for air side (h_a), and overall heat transfer coefficient for each slice and row of the heat exchanger. The simulation criteria was based on applying the same operating conditions of the experimental test rig for the object of validity of the theoretical prediction. It was decided to use two sets of experimental tests for the present heat exchanger in this work for the simulation validity. These were conducted at entering water temperature of (10) *°C* and (50) *°C* for water flow rate of (2000) *l/h* at three different air flow rates of (500), (1000) and (2000) *cfm*. For the performance validation, these tests were achieved at the same entering air temperature to the heat exchanger of (32) °C. More detailed experimental data can be found in Abdulrassol (2009)[18].

5-1 Heat Load for Heat Exchanger:

Figures (4-a) and (4-b) show the variation of heat exchanger load with the air flow velocity through the tube bank for water entering temperature of (10) *°C* and (50) *°C* respectively. The air velocity was ranged between (1.2) *m/s* and (4.6) *m/s* corresponding to (500) *cfm* and (2000) *cfm* air flow rates respectively. It is obvious that the heat load increases as the air flow rate increases. This is due to the improvement of the overall heat transfer coefficient of the heat exchanger by increasing the air side heat transfer coefficient. The heat load was increased by (4) and (3) times when the air velocity was raised from (1.2) *m/s* to (4.6) *m/s* for entering water temperature of (10) *°C* (Cooling Mode) and (50) *°C* (Heating Mode) respectively**.** This increase of the heat load due to the increasing trend of the heat transfer coefficient on the air side with air velocity as described by eq.(12). The percentage of increase was higher for the cooling mode than that of the heating mode due to the higher mean temperature difference between both heat exchanger streams.

The predicted and the experimental data showed almost the same trend with a good agreement for the (50) *°C* case with a maximum deviation of (2) % and quite higher for the (10) *°C* tests for the whole range of the experimental data.

5-2 Heat Transfer Coefficient for Air Side:

Figures (5-a) and (5-b) show a comparison for the heat transfer coefficient for air side between the theoretical prediction and the experimental data at various air velocities. These figures represent the behavior of the heat transfer coefficient variation with water flow rates of (2000) *l/hr*. It is obvious from these data that, the heat transfer coefficient values decrease with the low air velocity and it is lower when entering water at (10) *°C*.

The predicted values of the air side heat transfer coefficient showed the same behavior of that of the experimental data with a maximum deviation of (3%) as shown in figure (5). The heat transfer coefficient for both working modes of heating and cooling philosophy showed that increasing of flow velocity will improve (h_a) values having a values within (18-50) and (30-50) $W/m^2\ K$ for the cooling and heating modes respectively.

5-3 Overall Heat Transfer Coefficient

Figures (6-a) and (6-b) show the variation of the overall heat transfer coefficient for inlet water temperature of (10) *°C* and (50) *°C* respectively. The overall heat transfer coefficient of the heat exchanger for both of the cooling and heating modes varied between (17-47) $W/m^2\ K$ and (30-47) $W/m^2\ K$ respectively. Again, the predicted and calculated values from the experimental data showed a good agreement for both cooling and heating modes within less than (1%). The predicted values from computational model for the overall heat transfer coefficient along its depth (*D*) and along heat exchanger height (*H*) are shown in figure (7) for air flow rates of (2000) *cfm* at water entering temperature of (10) *°C* and (50) *°C*. It is obvious that the overall heat transfer coefficient of the heat exchanger did not change much and it is essentially a constant value.

5-4 Air Temperature Distribution:

Figure (8) shows the variation of the experimental and present model exit air temperature out of the heat exchanger with the air velocity. For both, cooling and heating modes of air side, the exit air temperature shows a trend of decreasing as the air velocity increases. Since increasing air velocity increases causes an increase in the air side heat transfer coefficient (h_a) and the (U_o) value which in turn produces higher heat exchanger load as shown in the figure. The maximum discrepancy between the present model prediction and experimental data for the whole range of the test conditions was less than (1%).

Figure (9) shows the exit air temperature distribution along its depth (*D*) and along the heat exchanger height (*H*) for air flow rates of (2000) *cfm* at water entering temperature (10) *°C* and (50) °C. For the cooling mode the temperature difference for the first row showed a

value of about twice that of the second row with (2.5) *°C* and (1.25) *°C* respectively, figure (9.a). The same behavior was also observed for the heating mode as it is revealed from figure (9.b), although it has different numerical exit air temperature from the heat exchanger.

5-5 Effect of Heat Exchanger Core Aspect Ratio (H/L)

The aspect ratio is defined as the ratio of the height (*H*) to the length (*L*) of the core for the heat exchanger. Since the model is based on the down flow type with the water tanks on top and bottom of the core, larger aspect ratio means relatively longer tubes. For a given range of the aspect ratio, the results showed that a heat exchanger with smaller aspect ratio can perform better than larger aspect ratio case as shown in figure (10). The pressure drop in the air side (Δp_a) was increased by changing the aspect ratio from (0.67 - 1) with the different core size ($L \times D \times H$). This is because at higher aspect ratio the frontal area decrease over which air side experiences more obstruction in the flow direction.

5-6 Effect of Heat Exchanger Depth

The effect of the number of rows of the heat exchanger and its depth on the performance profile of the heat exchanger criteria can be focused by the present model. Figure (11) shows the variation of the overall heat transfer coefficient along the heat exchanger depth for water flowing at the rate of (2000) *l/h*. This is for entering water temperature of (10) *°C* and air entering temperature of (32) *°C* at flow rate of (2000) *cfm*. The present model predicted a heat exchanger having the dimensions of (18 × 11 × 18) cm^3 to fulfill these requirements. This maldistribution of the overall heat transfer coefficient is mainly due to the variation of the air properties throughout the heat exchanger as the air proceeds deeper in the flow direction in the heat exchanger. Figure (12) shows the predicted exit air temperature distribution through the heat exchanger for the same operating conditions stated above as obtained by the present model. It is obvious that the temperature of air has a smooth gradual reduction towards the heat exchanger exit side. This will provide a powerful tool for the designer to furnish the temperature distribution on the air side.

6. Conclusions

The following represents the main findings of the present work:

1. A computational model for the performance prediction of the air-cooled heat exchanger has been developed.
2. To validate the model, the heat load performance of a typical air-cooled heat exchanger was simulated over a practical industrial ranges of the air velocity. The specifications of the test heat exchanger given in table (1).
3. The model suggested in the present work shows a good agreement with the experimental data with drawn from the tested heat exchanger. The maximum

discrepancy between the experimental data and those calculated by the model for overall performance was about (3%) for the given range of the simulated conditions.

4. The different core sizes ($L \times D \times H$) can be evaluated from the present model of the air-cooled heat exchanger according to the operating condition and specified geometry for both fin and tube side.

Table (1): The Present Work Heat Exchanger Geometry.

Parameter	Specification	Dimension
Core	Length (L)	550 mm
	Depth (D)	35 mm
	Height (H)	370 mm
	Total No. of Tubes	110
	No. of tubes/row	55
	No. of fins/ tube	256
	Transverse Distance (X_T)	9.92 mm
	Longitudinal Distance (X_L)	20.46 mm
Fin	Pitch (P_f)	1.46 mm
	Length (L_f)	7.52 mm
	Depth (D_f)	15.88 mm
	Thickness (t_f)	0.24 mm
Tube	Height (H_t)	2.4 mm
	Depth (D_t)	15.88 mm
	Thickness (t_t)	0.28 mm

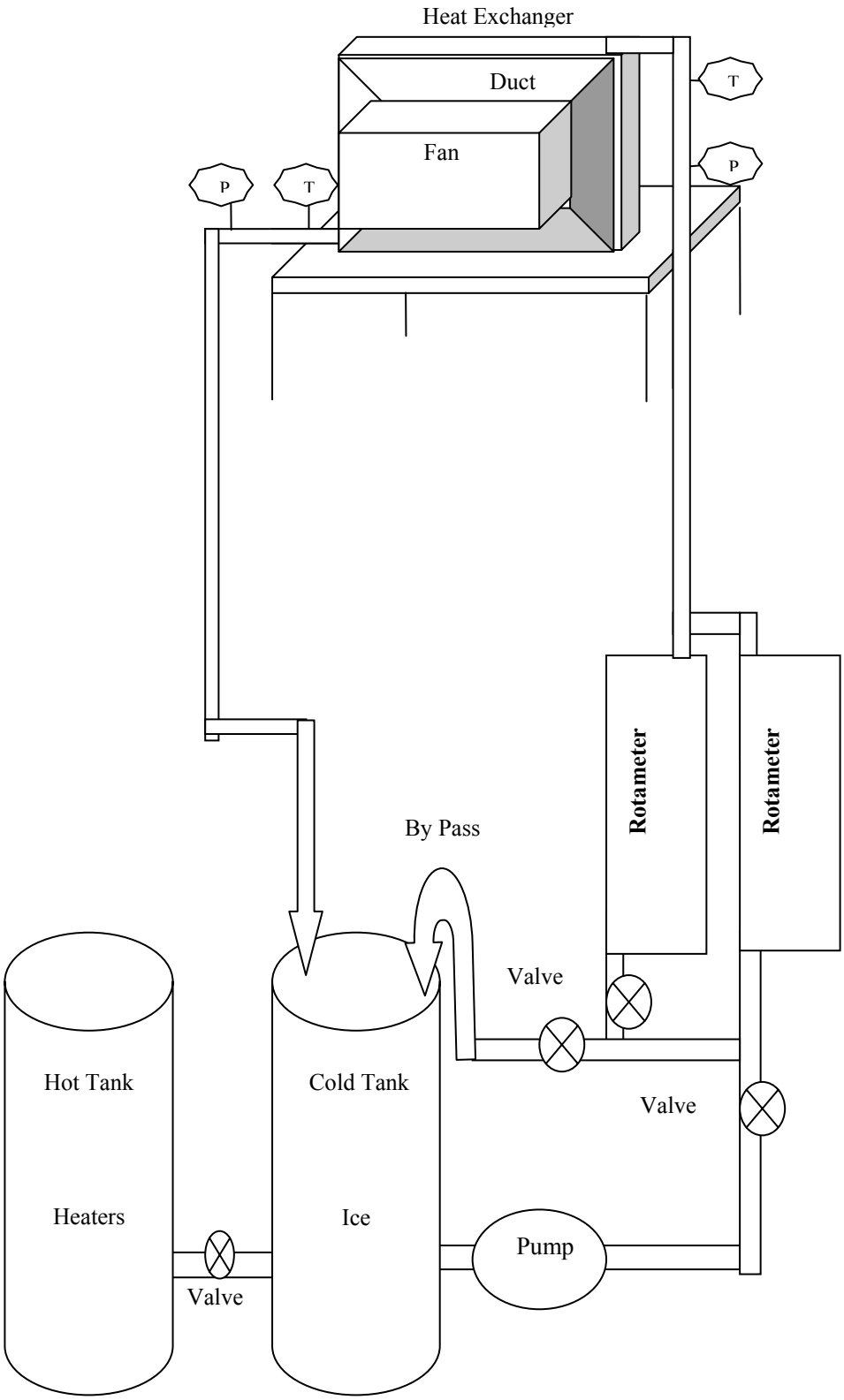

Figure (1): A Schematic Diagram of the Experimental Rig.

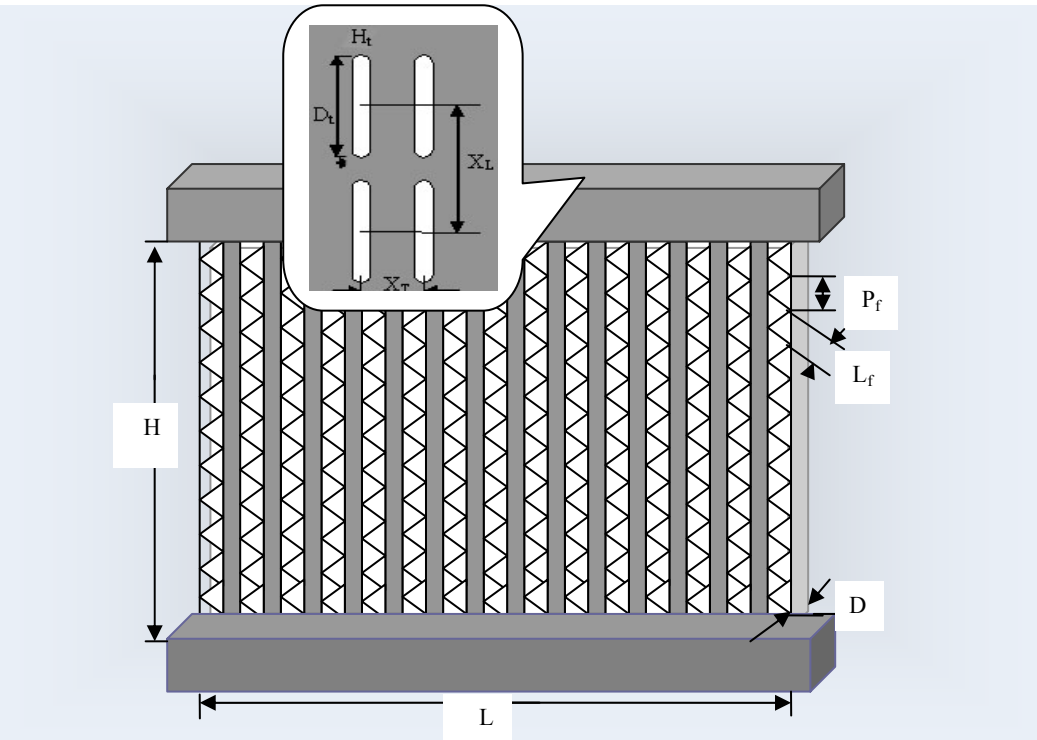

Figure (2): A View of Test Heat Exchanger Geometry.

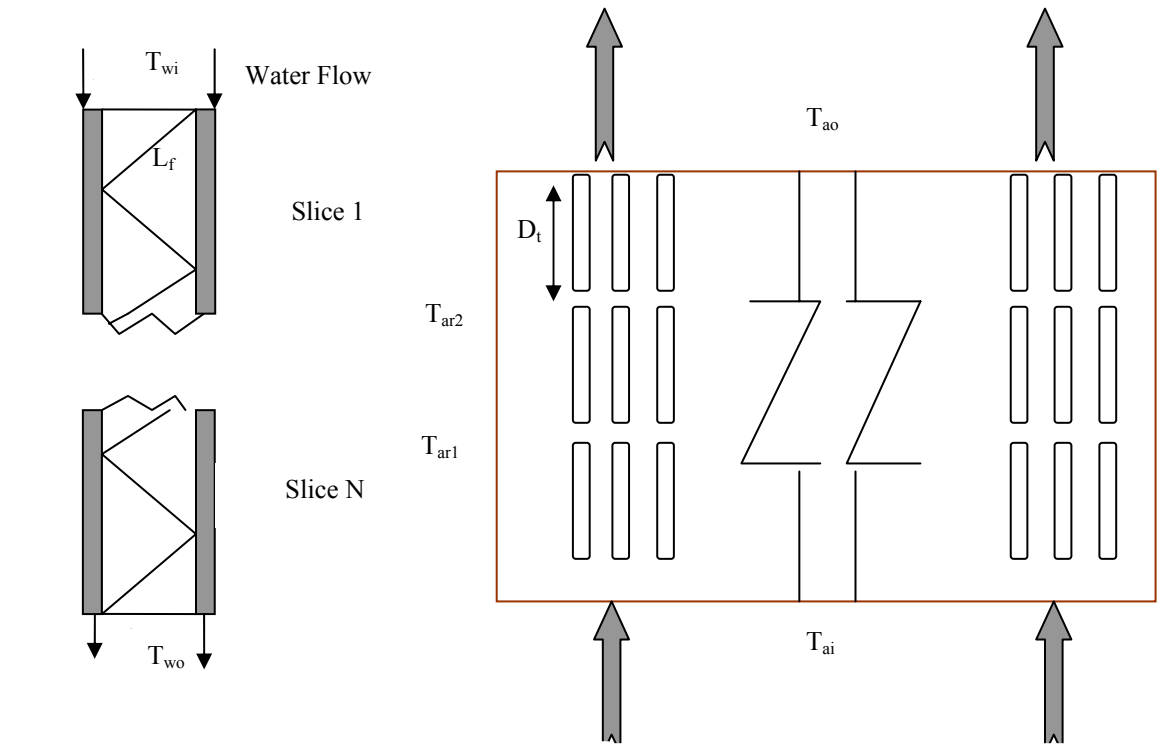

Figure (3-a) Slices for Single Tube Geometry

Figure (3-b) Model Heat Exchanger Arrangement

Figure (3): A Step by Step Marching Technique Model.

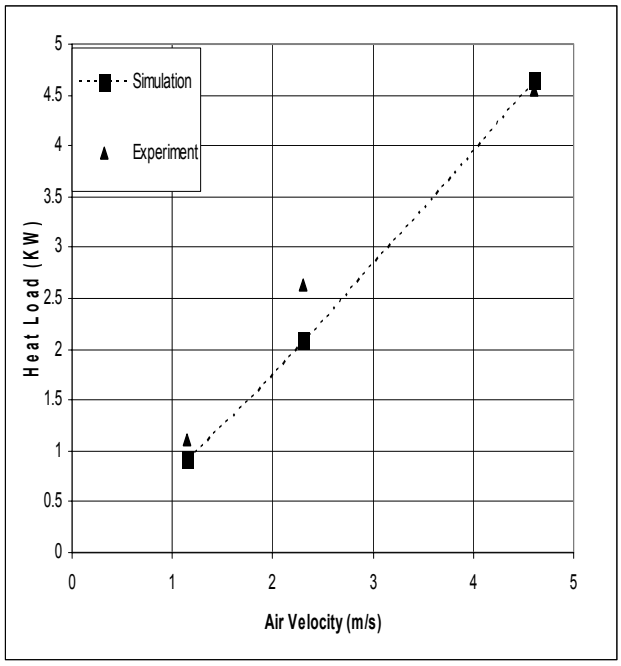

Fig (4-a) 10 °C inlet water temperature

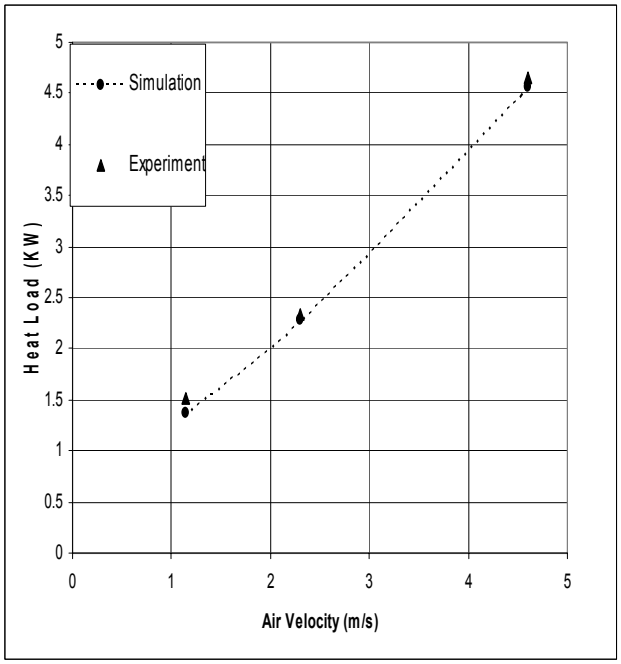

Fig (4-b) 50 °C inlet water temperature

Fig (4): Comparison between the Experimental and Present Model for the Effect of Air Velocity on Heat Load at Water Flow Rate 2000 (*l/h*).

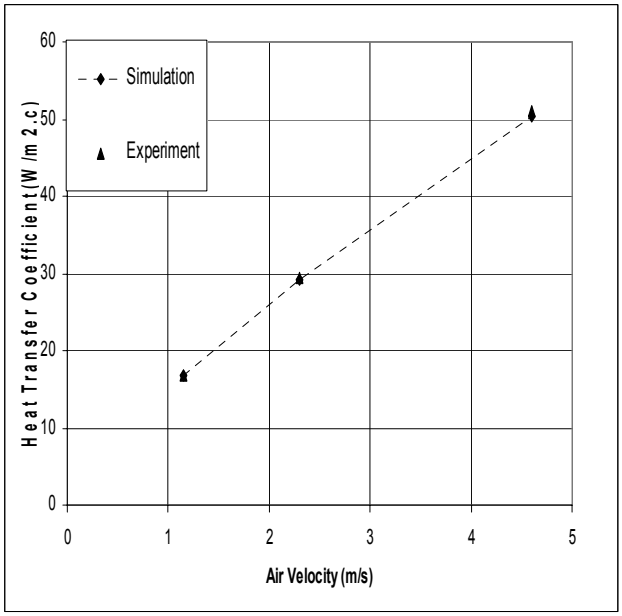

Fig (5-a) 10 °C inlet water temperature

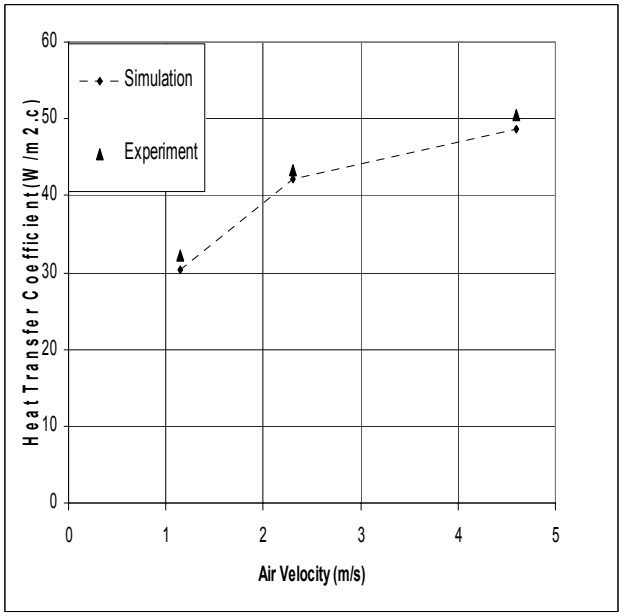

Fig (5-b) 50 °C inlet water temperature

Fig (5): Comparison between the Experimental and Present Model for the Effect of Air Velocity on Heat Transfer Coefficient ha, at Water Flow Rate 2000 (l/h).

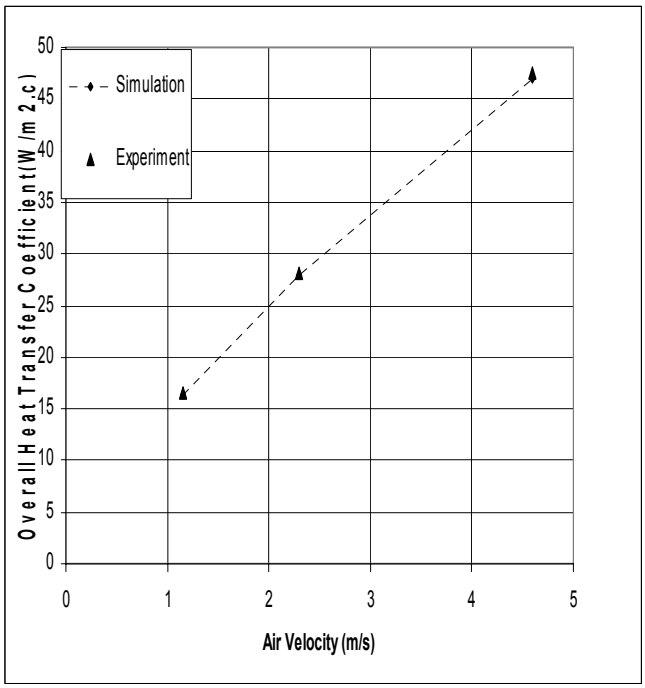

Fig (6-a) 10 °C inlet water temperature

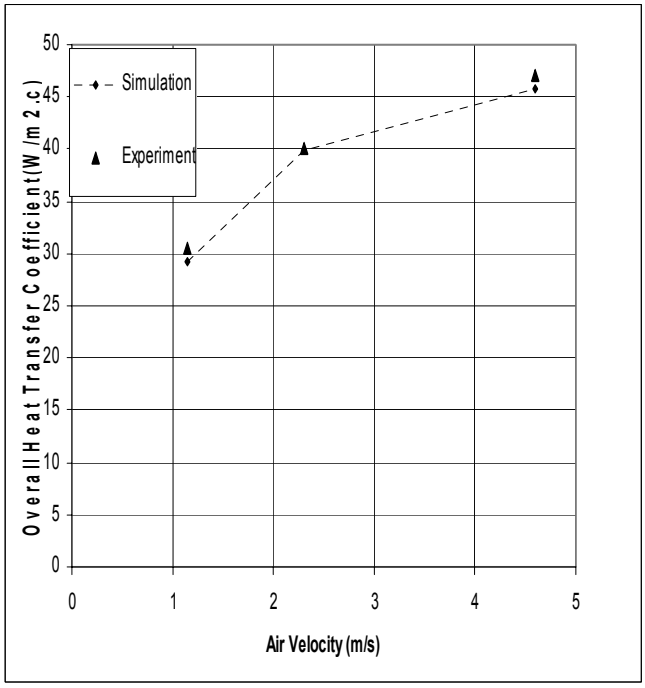

Fig (6-b) 50 °C inlet water temperature

Fig (6): A Comparison between the Experimental and Present Model Prediction for the Effect of Air Velocity on Overall Heat Transfer Coefficient at Water Rate Flow Rate 2000 *(l/hr)*.

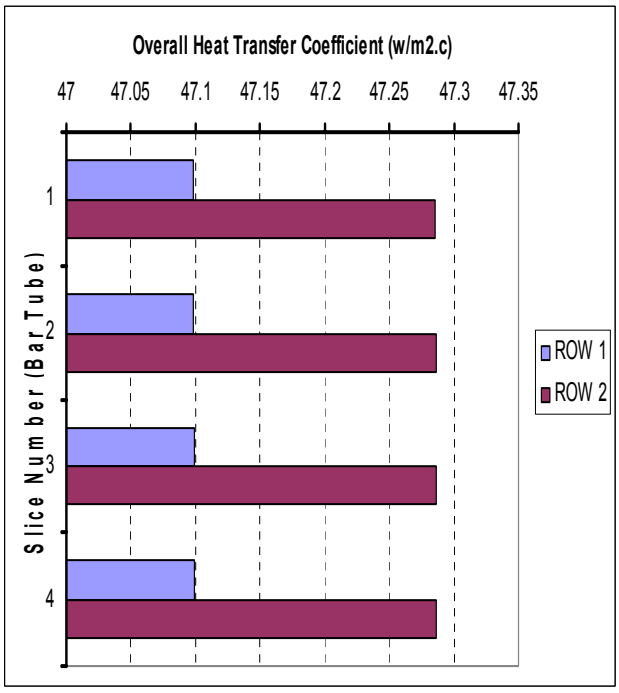

Fig (7-a) 10 °C inlet water temperature

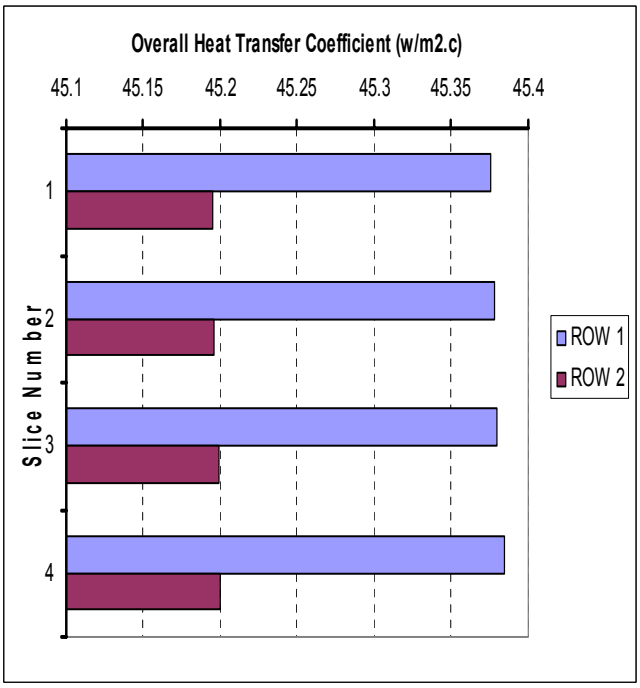

Fig (7-b) 50 °C inlet water temperature

Fig. (7): Overall Heat Transfer Coefficient Variation a long Heat Exchanger Height at Water Flow Rate of 2000 (l/h) and Air Flow Rate of 2000 *cfm*.

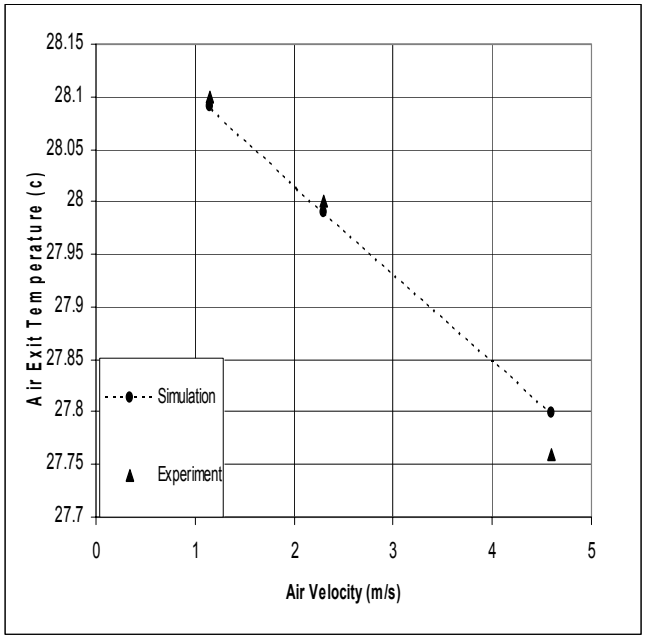

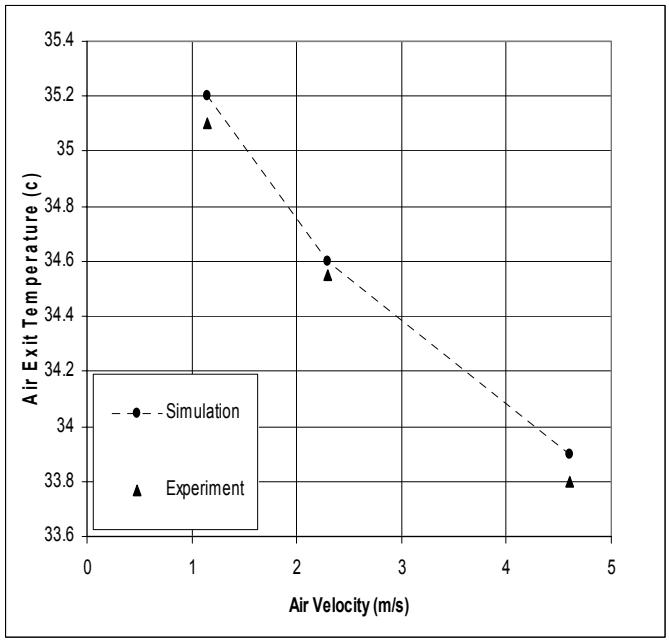

Fig (8-a) 10 °C inlet water temperature **Fig (8-b) 50 °C inlet water temperature**

Fig (8): Comparison between the Experimental and Present Model Prediction for the Effect of Air Velocity on Air Exit Temperature at Water Flow Rate of 2000 (l/h).

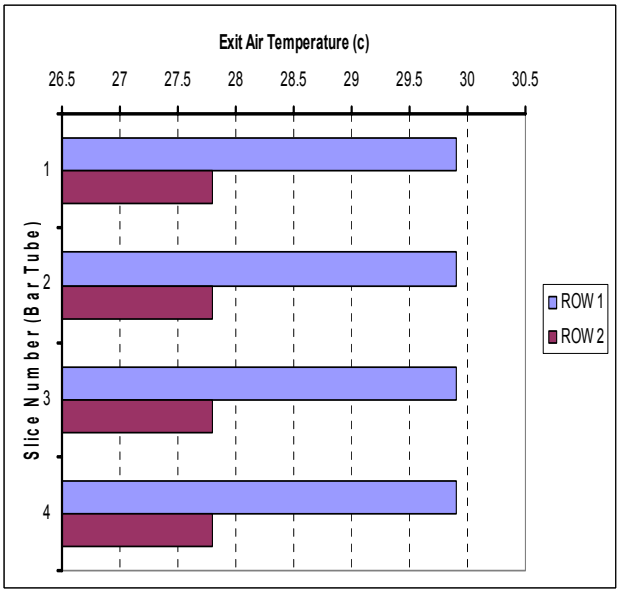

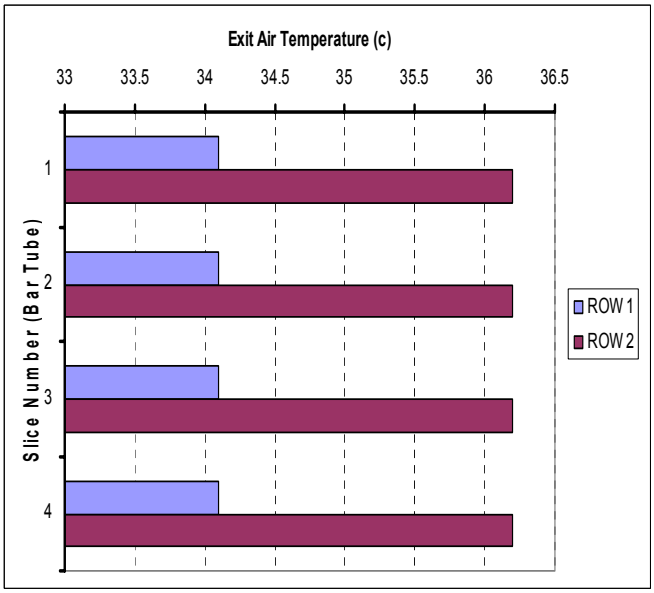

Fig (9-a) 10 °C inlet water temperature **Fig (9-b) 50 °C inlet water temperature**

Fig (9): Variation of Exit Air Temperature along Heat Exchanger Height at Water Flow Rate of 2000 (l/h) and Air Flow Rate of 2000 cfm.

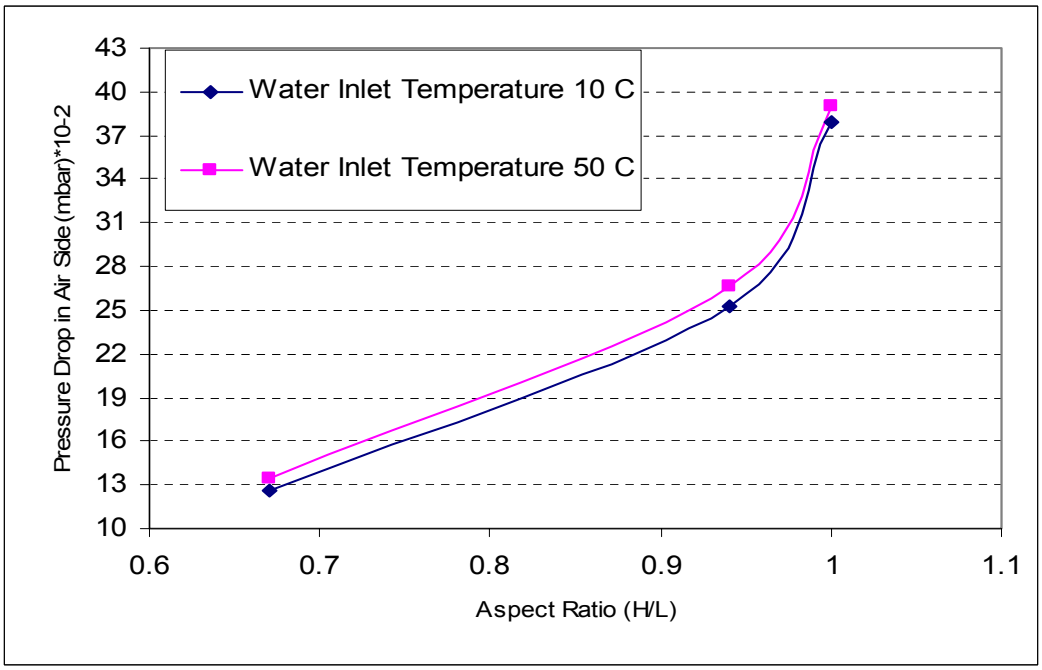

Fig (10): The Effect of Aspect Ratio (H/L) with Different Core Sizes (L × D × H) on the Pressure Drop in Air Side, Water Flow Rate of 2000 (l/h) and Air Flow Rate of 500 *cfm.*

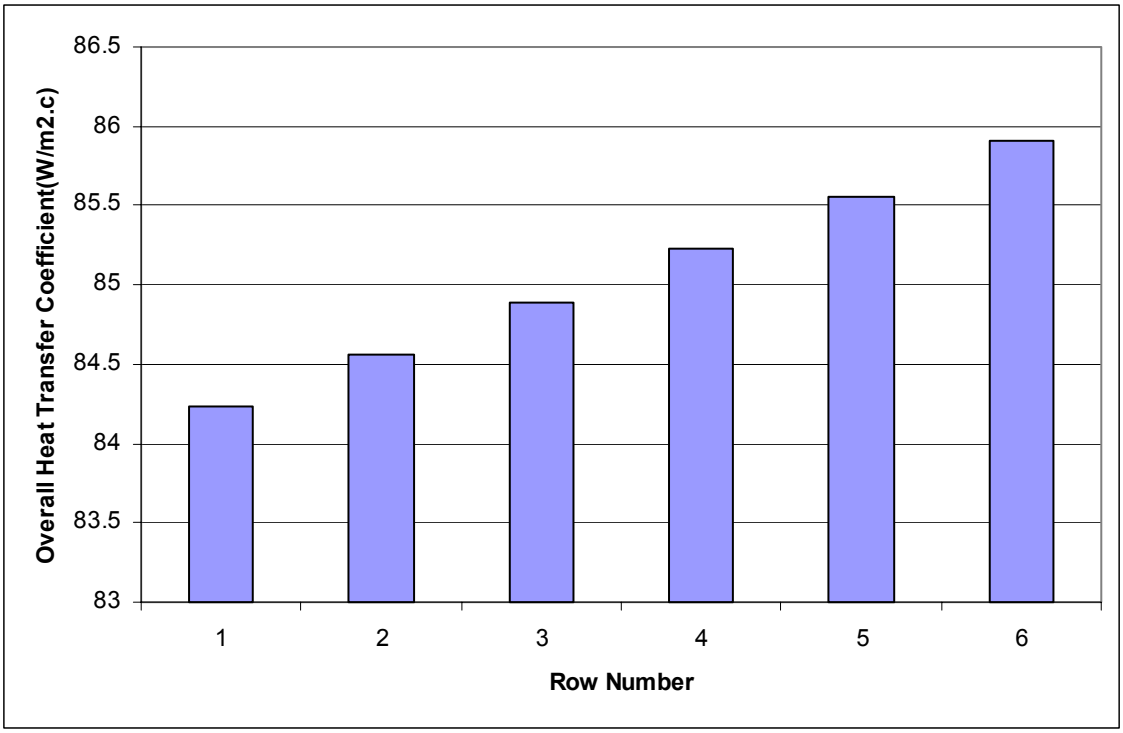

Fig(11): Variation of Overall Heat Transfer Coefficient a long Heat Exchanger Depth at Water Flow Rate of 2000 (l/h) with Entering Temp. 10 °C, and Air Flow Rate of 2000 cfm.

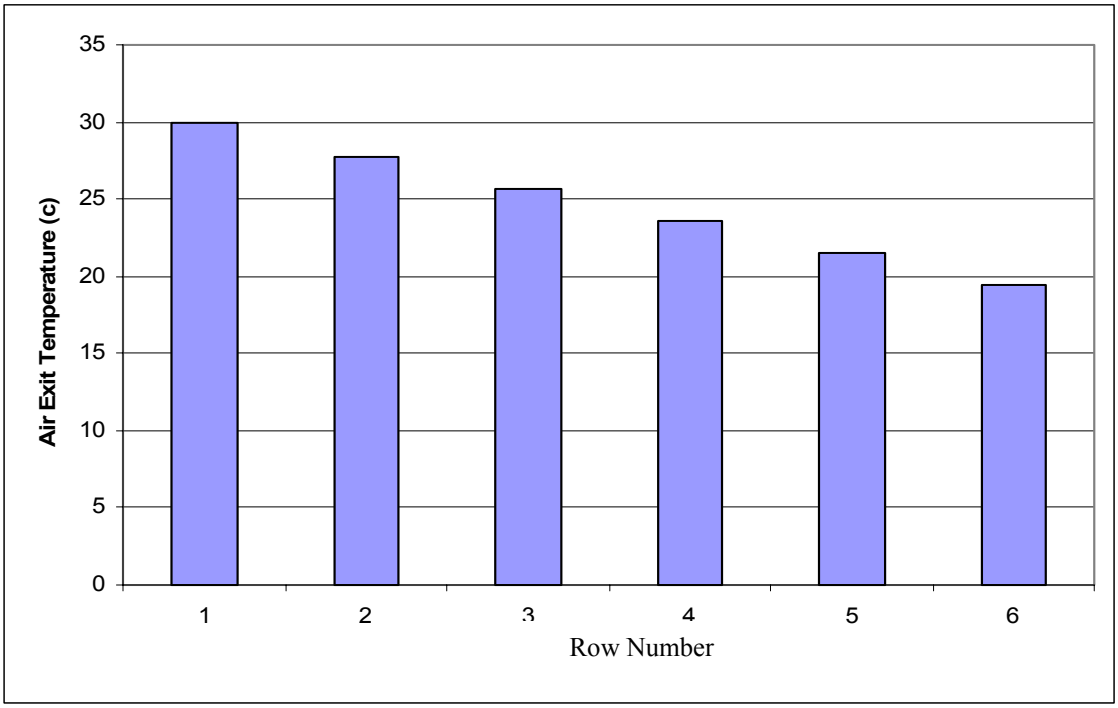

Fig. (12): Variation of Exit Air Temperature a long the Heat Exchanger Depth at Water Flow Rate of 2000 (l/h) and (10 °C) Inlet Temp., air flow rate of 2000 *cfm*.

7. References

1. Ganapathy,V., ***"Process-Design Criteria of Air Cooled Heat Exchangers"*** ,Chemical Engineering, pp. 418-425, McGraw-Hill Publication Book Co., New york,1979.
2. Hedderich, C.P., and Kellerher, M.D. ***"Design and Optimization of Air Cooled Heat Exchangers"***, Journal of Heat Transfer, Vol. 104, pp. 683-890, Nov. (1982).
3. Matthew, S., Layton, Joseph O'Hagan, ***"Comparison of Alternate Cooling Technologies for California Power Plants"***, Electric Power Research Institute (2002).
4. Dohoy, J. , Dennis, N***.," Numerical Modeling of Cross Flow Compact Heat Exchanger with Louvered Fins using Thermal Resistance Concept"*** SAE. Paper , 2006-01-0726, The University of Michigan**,** (2006).
5. Tarrad, A. H., Khudor, D. S., and Wahed, M.A***.," A Simplified Model for the Prediction of the Thermal Performance for Cross Flow Air Cooled Heat Exchangers with a New Air Side Thermal Correlation "***, Journal of Engineering and Development, Vol. 12, No.3, (2008).
6. Tarrad, A. H., and Mohammed, A. G., ***" A Mathematical Model for Thermo-Hydraulic Design of Shell and Tube Heat Exchanger Using a Step by Step Technique"*** Engineering and Development Journal, Vol. 10, No.4, December 2006.
7. Smith, E.M***.," Thermal Design of Heat Exchangers, a Numerical Approach"***, John Wiley and Sons, New York, (1997).
8. Hewitt, G.F., ***" Heat Exchanger Design Hand book"***, Begell House, New York, (1998).
9. Holman, J.,P., ***"Heat Transfer"*** , 7th edition, McGraw-Hill, New York(1989).
10. Dittus, F.W., and Boelter, L.M.K., Univ. Calif. (Berkeley) Pub. Eng., Vol.2, pp.443, (1930).
11. McAdams, W.H., ***"Heat Transmission"***, 3rd edition, McGraw-Hill, New York, (1954).
12. Adrian, B***.," Forced Convection: Internal Flows",*** Mechanical Engineering and Materials Science, Chap. 5, (2000).
13. Sieder, E.N., and Tate, C.E., ***"Heat Transfer and Pressure Drop of Liquids in Tubes"***, Ind. Eng. Chem., Vol.28, pp.1429, (1930).

14. Briggs D.E. and Young, E.H., ***"Convection Heat Transfer and Pressure Drop of Air Flowing Across Triangular Pitch Banks of Finned Tubes"***, Chem. Eng. Prog. Symp. Ser. Vol.59, No.41, pp1-10, (1963).

15. London, A. L***.," Compact Heat Exchanger-Design Methodology"***, edited by Kakac, S., Shah R. K. and Bergles, A. E., Hemisphere, New York, (1983).

16. Colburn, A. P***.," A Method of Correlating Forced Convection Heat Transfer Data and Comparison with Fluid Friction"***, Trans. AIChE, Vol 29, pp-174, (1933).

17. Bhatti, M.S. and Shah, R.K***.," Turbulent and Transition Flow Forced Convective Heat Transfer in Ducts"***, Single Phase Convective Heat Transfer, Wiley,(1987).

18. Abdulrasool, A.A***.," The Enhancement of Two-Shaft Gas Turbine Performance Using Improved Air Temperature"*** M.Sc. Thesis, AL-Mustansiriya University College of Engineering, (2009).

Nomenclature

Symbol	Description	Units
A	Transfer Surface Area	m²
A_f	Fin Area	m²
A_{cw}	Crosse Sectional Area of Water Side	m^2
A_{ca}	Crosse Sectional Area of Air Side	m^2
A_{exp}	Exposed Area of the Bare Tube	
Cp_a	Specific Heat Capacity of Dry Air	J/kg..k
Cp_w	Specific Heat Capacity of Water	J/kg..k
d_h	Hydraulic Diameter	m
D_t	Tube Depth	m
D_f	Fin Depth	m
D	Heat Exchanger Depth	m
G	Mass Velocity	Kg/(m^2 s)
h_a	Convection Heat Transfer Coefficient of Air Side	W/m².k
h_{fw}	Fouling Factor on the Water Side	W/m².k
h_w	Convection Heat Transfer Coefficient of Water Side	W/m².k
H_t	Tube Height	m
H	Heat Exchanger Height	m
k	Thermal Conductivity	W/(m ºK)
L_f	Fin Length	m

L	Heat Exchanger Length	m
$\dot{m}_a$	Air Mass Flow Rate	Kg/s
Nu	Nusselt Number	-
N_t	Number of Tubes	-
N_r	Number of Rows	-
P	Pressure	bar
$\dot{Q}$	Rate of Heat Transfer Lost or Gain	W
Re	Reynolds Number	-
T	Temperature	ºK
t_f	Fin Thickness	m
t_t	Tube Thickness	m
U_o	Overall Heat Transfer Coefficient	W/m².˚K
$\dot{V}$	Volumetric Flow Rate	m^3/s
v	Velocity	m/s
X_T	Transverse Space	m
X_L	Longitudinal Space	m

Greek Letters

η_o	$= 1 - \frac{A_f}{A}\left(1 - \eta_f\right)$ Overall Surface Efficiency
η_f	Fin Efficiency
ρ	Density (kg/m³)
λ_t	Perimeter of Tube Side (m)
λ_f	Perimeter of Fin (m)

Subscripts

a	Air
f	Fin
i	Input
o	Output
t	Tube
w	Water

Abbreviations

HVAC	Heating Ventilating and Air Conditioning
LMTD	Logarithmic Mean Temperature Difference